Publisher: GSA
Journal: GEOL: Geology
Article ID: G33863

Construction of an oceanic island: Insights from El Hierro 2011–12 submarine volcanic eruption

J. Rivera[1], G. Lastras[2], M. Canals[2]*, J. Acosta[1], B. Arrese[1], N. Hermida[1], A. Micallef[2], O. Tello[1], and D. Amblas[2]

[1]*Instituto Español de Oceanografía, Madrid E-28002, Spain*

[2]*GRC Geociències Marines, Universitat de Barcelona, Barcelona E-08028, Spain*

*E-mail: miquelcanals@ub.edu.

ABSTRACT

Eight consecutive swath bathymetry data sets were obtained to monitor the submarine eruption that occurred from October 10, 2011 to March 5, 2012 south of El Hierro Island, in the Canaries. An increase in seismic activity since July 2011 preceded the onset of the eruption marked by seismic tremor and stained waters. The first bathymetry 15 days after the eruption started depicts a cone topping at 205 m depth, growing on a pre-existing valley. Recurrent mapping evidences changes in the morphology and depth of the cone, allowing identifying collapses and calculating eruptive volumes and rates, which peaked at $12.7 \cdot 10^6$ $m^3 \cdot day^{-1}$ of non-dense rock equivalent (NDRE) in October 29–30. The final cone consists of at least four vents along a NNW-SSE lineation with the shallowest summit at 89 m depth. The total accumulated volume was $329 \cdot 10^6$ NDRE m^3, of which one third formed the cone. Similar cones have been identified on the submerged flanks of the island, with volumes ranging from $<50 \cdot 10^6$ to $>1000 \cdot 10^6$ NDRE m^3. As in many other volcanic islands, large-scale landslides play an important role in the evolution of El Hierro. A giant flank landslide (El Golfo, 13–134 ka, 150–180 km^3) mobilized in a single event a volume equivalent to 450–550 eruptions of the size of the reported

one, evidencing striking differences in the construction and destruction rates of the island. This study is relevant for future monitoring programs and geohazard assessment of new submarine eruptions.

INTRODUCTION

Most of Earth's volcanic activity occurs beneath the sea, at water depths exceeding 1000 m (Carey and Sigurdsson, 2007). Water depth is one of the main controls of submarine eruptions, together with magma supply, its composition and volatile content (McBirney, 1963; Head and Wilson, 2003). Volcanic activity in shallow water may result in explosive eruptions (Kokelaar and Durant, 1983) and tsunami generation (Latter, 1981). Tracking the depth of an eruption and how it evolves is essential for risk analysis. The recent eruption south of El Hierro Island, Canary Islands, from October 10, 2011 to March 5, 2012, resulted in a remarkable opportunity to monitor the growth of a newborn submarine volcano. In this paper we present eight swath bathymetry data sets obtained along this eruption and discuss its role in the evolution of the entire volcanic edifice. Surveys of an active submarine eruption have previously been conducted in Monowai cone, Kermadec Islands, within a frequency from 6 years to 14 days (Wright et al., 2008; Watts et al., 2012). High-frequency, repetitive multibeam monitoring of a single eruptive episode is unprecedented before the El Hierro 2011–12 eruption.

The Canary Islands chain, off Northwest Africa, originated in the early Miocene as the African plate moved over a mantle hotspot (Carracedo et al., 1998; Schmincke and Sumita, 2010). The islands show a general age progression from the eastern islands (>20 Ma) toward La Palma and El Hierro (<2 Ma) (Carracedo et al., 2002) (Fig. 1A). The oldest subaerial rocks in El Hierro and the only two known subaerial prehistoric eruptions (Tanganasoga and Montaña

Chamuscada) have been dated at 1.12 ± 0.02 Ma and ~4000 and 2500 years ago, respectively (Guillou et al., 1996).

El Hierro Island covers 273 km^2 and peaks at 1500 m above sea level. The whole volcanic edifice is 5500 km^3 and rises from 4000 m water depth (Schmincke and Sumita, 2010) (Fig. 1B). The island displays three large embayments (El Golfo, Las Playas and El Julan, Fig. 1B) resulting from large flank collapses during the last 200 ka that involved ~10% of its volume (Gee et al., 2001). These embayments are separated by three topographically elevated volcanic rift zones (Carracedo, 1994) defined by fissuring, faulting and aligned eruptive centers, which continue offshore. The submarine extension of the Southern Rift (Fig. 1B) consists of narrow volcanic lobes trending NE to SW that extend to a depth of 2500 m (Acosta et al., 2003), with many non-eroded cones at the top.

The El Hierro 2011–12 Eruption

A sudden increase of seismic activity began in July 2011 (IGN, 2012), which obliged the authorities to issue a first alert. The seismic crisis peaked on August 21 (454 events), but magnitudes continued to increase and a yellow alert was declared on September 23, 2011. The number of earthquakes exceeded 12,500 for the whole event (Fig. 1C). Very shallow earthquakes on October 9, seismic tremor and the presence of dead fish and a water stain south of La Restinga on October 10 indicated the onset of a submarine eruption in the Southern Rift of El Hierro (Fig. 1B and C) (Carracedo et al., 2012). Red alert was declared on October 11. The eruption, of basaltic character (Carracedo et al., 2012), continued based on seismic tremor and stained waters, and decreased gradually until March 6, 2012, when the alert was removed.

METHODS

From October 22, 2011 to February 24, 2012, six surveys on board *R/V Ramón Margalef* focused on changes in seabed elevation and water column using acoustic techniques. Bathymetry data were acquired with an EM710 echo sounder. Real-time surface sound-velocity corrections were conducted using a Micro SV probe, whereas water column corrections were based on SVPlus V2 sound-velocity profiles obtained on a sub-daily basis. Processed bathymetric grid cell size is 10 m. The first survey mapped the new volcanic edifice and its surroundings on October 25, 2011 (Figs. 2A and S1C), October 29 (Fig. S1D) and October 31 (Fig. S1E); successive surveys were conducted on November 13 (Figs. 2B and S1F), December 2 (Figs. 2C and S1G), January 11, 2012 (Fig. S1H), February 8 (Fig. S1I) and February 24 (Figs. 2D and S1J).

Instituto Hidrográfico de la Marina (IHM) made available pre-eruption, multibeam-derived bathymetry for the flanks of El Hierro (Figs. 1B and S1B). Out of the eruption area, all data sets are coincident, except this IHM bathymetry, which displays a mean depth diminution of 26.4 m (standard deviation is 15.8 m) with respect to the other data sets. Such differences have been treated as a static error in volumetric calculations and corrected accordingly.

The water column was acoustically surveyed using an EK60 echo sounder, which operates at six different frequencies yielding volume backscattering coefficient in decibels (or reflectivity) and imaging emission spots and plumes (Fig. S2). Vessel positioning was ensured by a DGPS system with EUSAT differential correction by OmniSTAR, yielding a horizontal accuracy within ± 15 cm.

Non-dense rock equivalent (NDRE) volumes (e.g., the volumes of volcanic material accumulated without porosity corrections needed to calculate the volume of erupted magma), and rates during the eruption were calculated computing depth changes for each 10x10 m cell between two consecutive data sets. If a cell was not surveyed during a given survey, depth

change was calculated with respect to the temporally closest data set and proportionally attributed, taking into account the lapsed time between the two data sets used. Extreme values in depth changes caused by acquisition artifacts were corrected. Volumes of 221 older submarine volcanic cones were calculated by simplifying each edifice to an ideal cone with a basal area equal to the area occupied by the cone and a height equal to the difference between the summit depth and the mean depth of the area perimeter.

THE SEAFLOOR EXPRESSION

The first bathymetric survey (Fig. 2A), 15 days after the eruption started, depicts a volcanic cone located at 27º37.12'N and 17º59.48'W, whose summit was masked by an eruptive plume (Figs. S1 and S2). The shallowest surveyed point on the cone was at 205 m water depth; the same point was at 363 m (corrected) depth before the eruption. In this first survey, the cone, $33 \cdot 10^6$ NDRE m^3 in volume, was developing within a pre-existing valley (Figs. 1B and 3A) in the western flank of the Southern Rift of El Hierro. The valley directed the lava flow toward an apron at depths exceeding 1000 m, which by then had accumulated $57 \cdot 10^6$ NDRE m^3 of lava (Figs. 1B and 3B). The eruptive plume in the water column was advected southwestwards following the dominant path of the Canary Current.

The cone growth in a sloping area contributed to instability. Cone deconstruction occurred between October 25 and 29 (Figs. 3 and S1) and again between October 31 and November 13 (Figs. 2B and 3). During both episodes, the cone's height and volume decreased while the apron accumulated new material. Contrastingly, during the first episode, cone height decreased uniformly, probably indicating deflation or collapse of a shallow magmatic chamber; during the second, height decreased only for the southwestern flank, suggesting cone instability

and sliding of a large block (Figs. 2B and 3A). Eruption rates peaked after the first collapse, with a value of $12.7 \cdot 10^6$ NDRE $m^3 \cdot day^{-1}$ during October 29 and 30.

The November 13 bathymetry (Fig. 2B) revealed that the eruption, which continued generating a plume in the water column (Fig. S2), was occurring through two vents, the second growing to the northwest. 53 days after the start of the eruption (December 2) (Fig. 2C), the two vents developed into a double cone almost infilling the upper part of the valley. Between November 13 and December 2, failure at the lower part of the valley took place, with valley walls affected by small-scale landsliding (Fig. 2B and C). Subsequent bathymetries indicate that the cone continued growing and that its summit moved gradually to the northwest (Fig. S1).

The February 24, 2012 bathymetry, 137 days after the eruption onset, shows that the double cone, which was eroded by small landslides (Fig. 2D), developed into a fissure eruption with at least four attached vents following a NNW-SSE lineation (Fig. 3A); the shallowest summit was at 89 m water depth. Eruption rates had decreased since January (Fig. 3B), as also shown by the fainter plume (Fig. S2), probably indicating that only degassing was occurring at that time. The accumulated volume throughout the eruption was $329 \cdot 10^6$ NDRE m^3, one third of which represents the cone build-up and valley infill (Fig. 3B). No data are available to account for volumes accumulated in the lower apron or for material transported away within the water column.

DISCUSSION AND CONCLUSIONS

In addition of the new cone, several other cones, both larger and smaller in volume, can be identified in the Southern Ridge (Figs. 2D and S3). Some are multi-vent too, probably fissure-fed, aligned along a NNW-SSE direction, i.e., following the structural trend of the Ridge and of the 2011–12 event seismicity (Fig. 1). Some cones are located at valley headwalls similarly to

the 2011–12 eruption (Fig. 2A and D). Alike valleys, described as downslope-facing horseshoe-shaped scarps, have been attributed to small-scale flank collapses in active volcanoes, such as Kick'em Jenny volcano, Grenada (Lindsay et al., 2005), or Monowai cone, Kermadec Islands, where repeated surveys have evidenced the growth of a cone within a scarp (Wright et al., 2008).

The new cone adds to a large number of similar structures both on land and offshore in the flanks of El Hierro. A total of 221 submarine cones have been identified over an area of 6100 km^2, with volumes ranging from $<50 \cdot 10^6$ to $>1000 \cdot 10^6$ NDRE m^3 (Fig. S3). In rough numbers, the 2011–12 eruption is an addition of 0.006% to the volume of the edifice (5500 km^3) (Schmincke and Sumita, 2010). Assuming that half of the 1.12-Ma-old edifice is formed by extrusive rocks, and that 450 km^3 of rock have been removed by flank collapse in the past, some 9,000 similar eruptions are needed to build it up with a recurrence interval of 125 years.

The El Hierro 2011–12 eruption lasted 138 days, most likely representing a typical growth episode of the island. Volcanic islands undergo periods of destruction through large-scale flank collapses, such as those represented by El Golfo, El Julan and Las Playas; medium-scale collapses of ridge flanks, such as the eastern flank of the Southern Ridge, as evidenced by split cones in the new bathymetry (Figs. 2D and S3); or small-scale collapses, such as the partial collapse of the new cone during the eruption or, likely, the valley in which it formed. Large-scale collapses mobilized ~450 km^3 of El Hierro during the last 200–300 thousand years, with each landslide involving ~3% of the edifice volume (Gee et al., 2001). A giant flank landslide such as El Golfo debris avalanche (150–180 km^3, 13–134 ka) (Masson, 1996) mobilized in a single event a volume equivalent to 450–550 eruptions similar in size to the recent one.

The above data suggest that while volcanic growth in El Hierro, and likely in other volcanic islands in equivalent geological settings worldwide, proceeds in terms of eruptive episodes producing modest volumes of rock spaced at least by a century, its destruction occurs, to a large extent, as a consequence of massive flank collapses. While evidence of massive debris avalanche deposits has been found in a number of locations, the El Hierro 2011–12 submarine eruption represents a rare occasion to observe how these islands are built. The morphological and volumetric evolution of the El Hierro submarine volcano reported here could be useful for guiding future monitoring programs and geohazard assessment. At the moment of writing (late June 2012) seismic activity and ground deformation had reactivated.

ACKNOWLEDGMENTS

IEO provided financial and shiptime support (Bimbache project). Generalitat de Catalunya is acknowledged (2009-SGR-1305). AM is a Marie Curie researcher (PIEF-GA-2009-252702). We thank the crew of R/V Ramón Margalef for their courage in collecting the data. Two anonymous reviewers and J. Carracedo helped improving the manuscript.

REFERENCES CITED

Acosta, J., Uchupi, E., Smith, D., Muñoz, A., Herranz, P., Palomo, C., Llanes, P., and Ballesteros, M., and ZEE Working Group, 2003, Comparison of volcanic rifts on La Palma and El Hierro, Canary Islands and the Island of Hawaii: Marine Geophysical Researches, v. 24, p. 59–90, doi:10.1007/s11001-004-1162-6.

Carey, S., and Sigurdsson, H., 2007, Exploring submarine arc volcanoes: Oceanography, v. 20, p. 80–89.

Carracedo, J.C., 1994, The Canary Islands: An example of structural control on the growth of large oceanic-island volcanoes: Journal of Volcanology and Geothermal Research, v. 60, p. 225–241, doi:10.1016/0377-0273(94)90053-1.

Carracedo, J.C., Day, S., Guillou, H., Rodríguez Badiola, E., Cañas, J.A., and Pérez-Torrado, F.J., 1998, Hotspot volcanism close to a passive continental margin: The Canary Islands: Geological Magazine, v. 135, p. 591–604, doi:10.1017/S0016756898001447.

Carracedo, J.C., Pérez, F.J., Ancochea, E., Meco, J., Hernán, F., Cubas, C.R., Casillas, R., Rodríguez, E., and Ahijado, A., 2002, Cenozoic volcanism II: The Canary Islands, *in* Gibbons, W., and Moreno, T., eds., The Geology of Spain: Geological Society of London, p. 439–472.

Carracedo, J.C., Pérez-Torrado, F.J., Rodríguez-González, A., Fernández-Turiel, J.L., Klügel, A., Troll, V.R., and Wiesmaier, S., 2012, The ongoing volcanic eruption of El Hierro, Canary Islands: Eos [Transactions, American Geophysical Union], v. 93, p. 89–90, doi:10.1029/2012EO090002.

Gee, M.J.R., Watts, A.B., Masson, D.G., and Mitchell, N.C., 2001, Landslides and the evolution of El Hierro in the Canary Islands: Marine Geology, v. 177, p. 271–293, doi:10.1016/S0025-3227(01)00153-0.

Guillou, H., Carracedo, J.C., Pérez-Torrado, F., and Rodríguez Badiola, E., 1996, K-Ar ages and magnetic stratigraphy of a hotspot-induced, fast-grown oceanic island: El Hierro, Canary Islands: Journal of Volcanology and Geothermal Research, v. 73, p. 141–155, doi:10.1016/0377-0273(96)00021-2.

Head, J.W.I., and Wilson, L., 2003, Deep submarine pyroclastic eruptions: Theory and predicted landforms and deposits: Journal of Volcanology and Geothermal Research, v. 121, p. 155–193, doi:10.1016/S0377-0273(02)00425-0.

IGN, 2012, Boletín de El Hierro: http://www.ign.es/ign/resources/volcanologia/txt/boletin_HIERRO.txt (last accessed March 2012).

Kokelaar, B.P., and Durant, G.P., 1983, The submarine eruption and erosion of Surtla (Surtsey), Iceland: Journal of Volcanology and Geothermal Research, v. 19, p. 239–246, doi:10.1016/0377-0273(83)90112-9.

Latter, J.H., 1981, Tsunamis of volcanic origin: Bulletin of Volcanology, v. 44, p. 467–490, doi:10.1007/BF02600578.

Lindsay, J.M., Shepherd, J.B., and Wilson, D., 2005, Volcanic and scientific activity at Kick 'em Jenny submarine volcano 2001–2002: Implications for volcanic hazard in the Southern Grenadines, Lesser Antilles: Natural Hazards, v. 34, p. 1–24, doi:10.1007/s11069-004-1566-2.

Masson, D.G., 1996, Catastrophic collapse of the flank of El Hierro about 15,000 years ago, and the history of large flank collapses in the Canary Islands: Geology, v. 24, p. 231–234, doi:10.1130/0091-7613(1996)024<0231:CCOTVI>2.3.CO;2.

McBirney, A.R., 1963, Factors governing the nature of submarine volcanism: Bulletin of Volcanology, v. 26, p. 455–469, doi:10.1007/BF02597304.

Schmincke, H.U., and Sumita, M., 2010, Geological Evolution of the Canary Islands: Koblenz, Germany, Görres-Verlag, 200 p.

Watts, A.B., Peirce, C., Grevemeyer, I., Paulatto, M., Stratford, W., Bassett, D., Hunter, J.A., Kalnins, L.M., and de Ronde, C.E.J., 2012, Rapid rates of growth and collapse of Monowai submarine volcano in the Kermadec Arc: Nature Geoscience, v. 5, p. 510–415, doi:10.1038/ngeo1473.

Wright, I.C., Chadwick, W.W., Jr., de Ronde, C.E.J., Reymond, D., Hyvernaud, O., Gennerich, H.H., Stoffers, P., Mackay, K., Dunkin, M.A., and Bannister, S.C., 2008, Collapse and reconstruction of Monowai submarine volcano, Kermadec arc, 1998–2004: Journal of Geophysical Research, v. 113, B08S03, doi:10.1029/2007JB005138.

FIGURE CAPTIONS

Figure 1. A: Age of the Canary Islands (Carracedo et al., 2002). B: Topo-bathymetric map of El Hierro. Locations of main geographical references and Figure 2 are provided. The main components of the 2011–12 eruption and resulting deposits are depicted. Pre-eruption bathymetry is from IHM. C: Location of earthquakes from July 19, 2011 to March 6, 2012 (IGN, 2012).

Figure 2. Four of the eight successive multibeam bathymetries obtained during the eruption. A: October 25, 2011. B: November 13, 2011. C: December 2, 2011. D: February 24, 2012. Unsurveyed areas are shown in gray. Changes in depth values over or below 5% with respect to the previous survey are outlined in B, C and D in black (depth decrease: inflation or deposition) and red (depth increase: deflation or erosion). In A, depth change is with respect to IHM bathymetry (Fig. 1C) after correcting static error. In D, the volcanic cone and the canyon and apron areas used in the volumetric calculations (Fig. 3B) are depicted.

Figure 3. A: Bathymetric cross-sections of El Hierro 2011–12 cone during the eruption. The last bathymetry (February 24, 2012) displays four successive vents in a NNW-SSE direction. Note

the difference between IHM data and the other data sets outside the new cone, which has been corrected for the volumetric calculations. B: Non-dense rock equivalent (NDRE) accumulated volumes and rates during the eruptive episode within the cone and the upper apron areas.

[1]GSA Data Repository item 2013xxx, consisting on Supplementary Figs. S1 (3D views of the eight bathymetries), S2 (EK60 echograms displaying backscatter in the water column) and S3 (location and volumes of other cones identified in El Hierro edifice), is available online at www.geosociety.org/pubs/ft2013.htm, or on request from editing@geosociety.org or Documents Secretary, GSA, P.O. Box 9140, Boulder, CO 80301, USA.

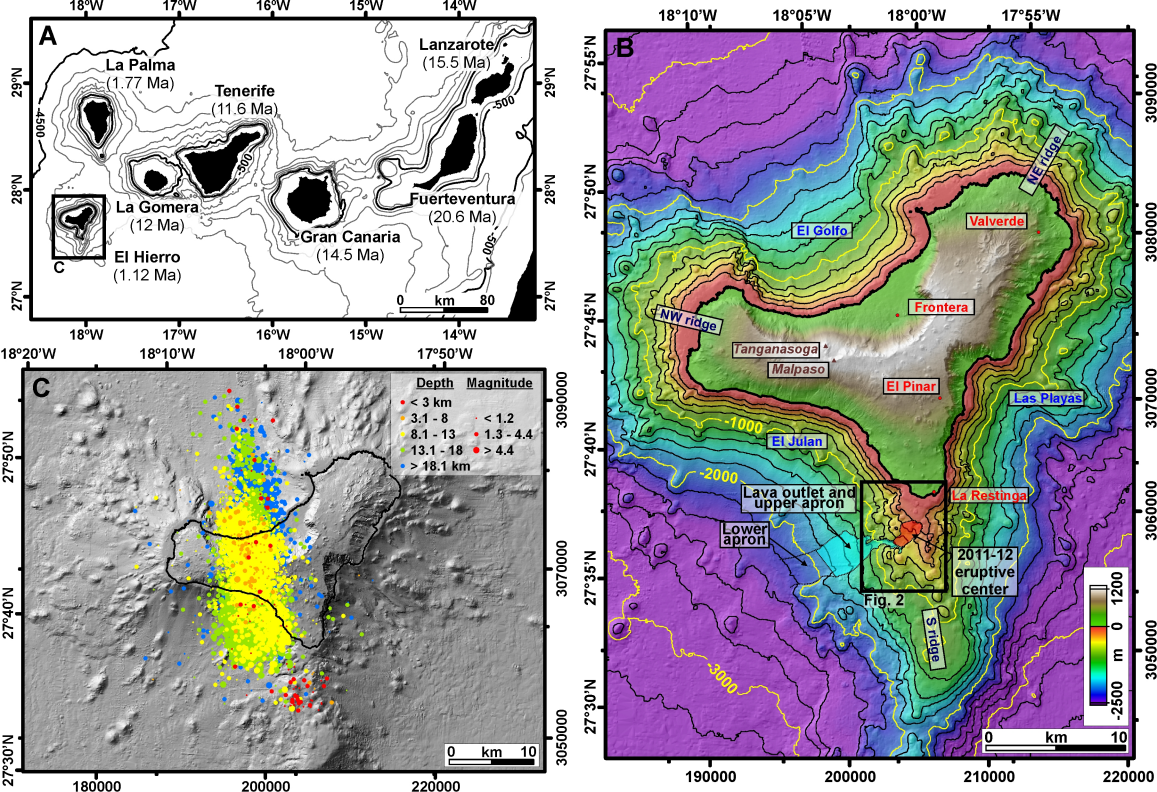
A
La Palma
(1.77 Ma)
Tenerife
(11.6 Ma)
Lanzarote
(15.5 Ma)
La Gomera
(12 Ma)
El Hierro
(1.12 Ma)
Gran Canaria
(14.5 Ma)
Fuerteventura
(20.6 Ma)
C
0 km 80
18°W
17°W
16°W
15°W
14°W
29°N
28°N
27°N
B
18°10'W
18°05'W
18°00'W
17°55'W
27°55'N
27°50'N
27°45'N
27°40'N
27°35'N
27°30'N
3090000
3080000
3070000
3060000
3050000
NE ridge
El Golfo
Valverde
Frontera
NW ridge
Tanganasoga
Malpaso
El Pinar
Las Playas
-1000
El Julan
-2000
Lava outlet and upper apron
La Restinga
Lower apron
2011-12 eruptive center
Fig. 2
S ridge
-3000
m
1200
0
-2500
0 km 10
190000
200000
210000
220000
C
18°20'W
18°10'W
18°00'W
17°50'W
Depth
< 3 km
3.1 - 8
8.1 - 13
13.1 - 18
> 18.1 km
Magnitude
< 1.2
1.3 - 4.4
> 4.4
0 km 10
180000
200000
220000

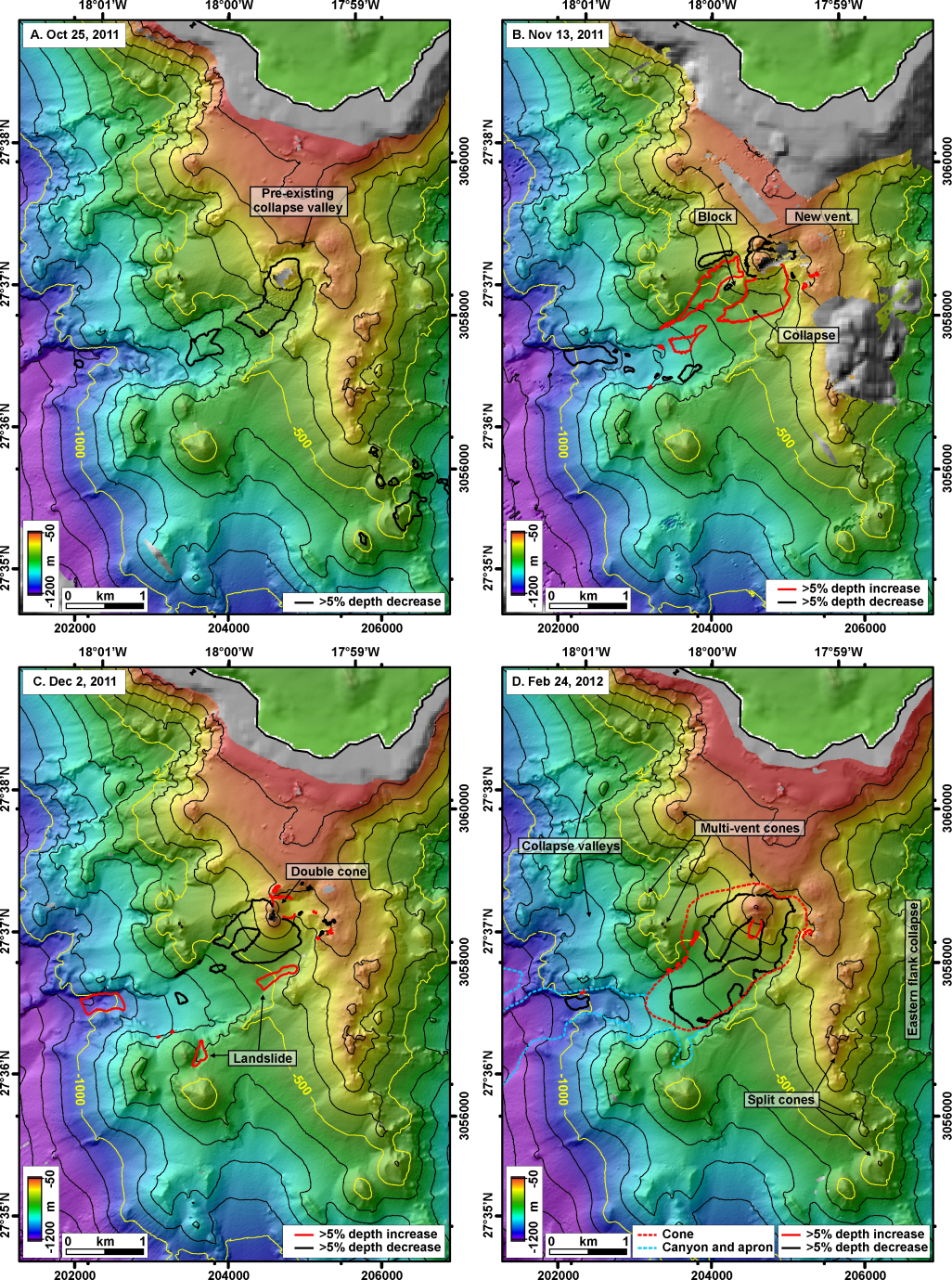
A. Oct 25, 2011
Pre-existing collapse valley
-1000
-500
-1200 m -50
0 km 1
>5% depth decrease
B. Nov 13, 2011
Block
New vent
Collapse
>5% depth increase
>5% depth decrease
C. Dec 2, 2011
Double cone
Landslide
D. Feb 24, 2012
Collapse valleys
Multi-vent cones
Eastern flank collapse
Split cones
Cone
Canyon and apron
18°01'W
18°00'W
17°59'W
27°38'N
27°37'N
27°36'N
27°35'N
202000
204000
206000
3060000
3058000
3056000

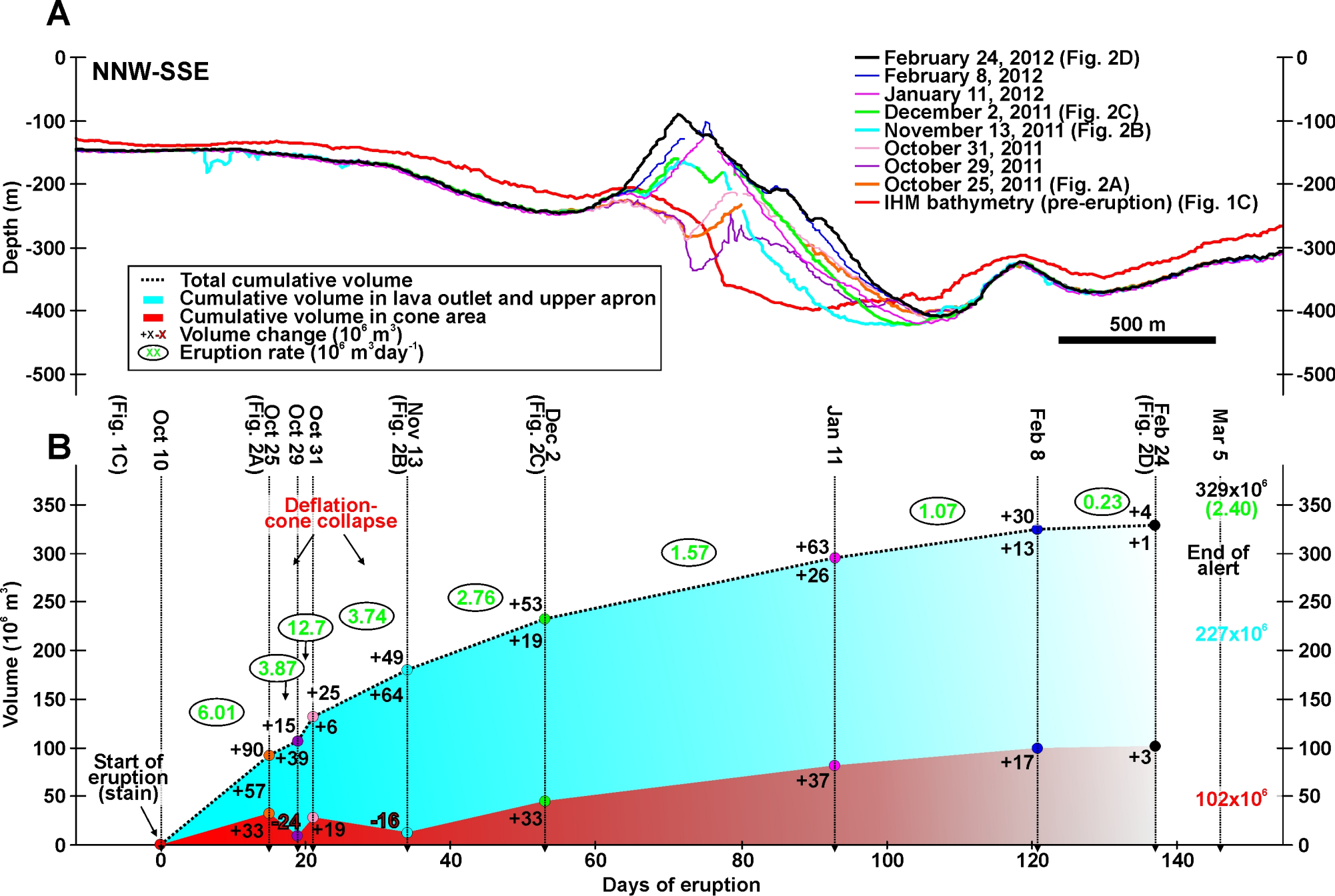
A
NNW-SSE
Depth (m)
0
-100
-200
-300
-400
-500
February 24, 2012 (Fig. 2D)
February 8, 2012
January 11, 2012
December 2, 2011 (Fig. 2C)
November 13, 2011 (Fig. 2B)
October 31, 2011
October 29, 2011
October 25, 2011 (Fig. 2A)
IHM bathymetry (pre-eruption) (Fig. 1C)
Total cumulative volume
Cumulative volume in lava outlet and upper apron
Cumulative volume in cone area
+x-x Volume change (10^6 m^3)
xx Eruption rate (10^6 m^3 day^-1)
500 m
B
Oct 10 (Fig. 1C)
Oct 25 (Fig. 2A)
Oct 29
Oct 31
Nov 13 (Fig. 2B)
Dec 2 (Fig. 2C)
Jan 11
Feb 8
Feb 24 (Fig. 2D)
Mar 5
Deflation-cone collapse
Start of eruption (stain)
6.01
3.87
12.7
3.74
2.76
1.57
1.07
0.23
+90
+57
+15
+39
+25
+6
+49
+64
+53
+19
+63
+26
+30
+13
+4
+1
+33
+24
+19
-16
+33
+37
+17
+3
329x10^6
(2.40)
End of alert
227x10^6
102x10^6
Volume (10^6 m^3)
Days of eruption
0
20
40
60
80
100
120
140
350
300
250
200
150
100
50
0

SUPPLEMENTARY FIGURE CAPTIONS

Figure S1. 3D views of eight successive multibeam bathymetries obtained during the eruption. A: General view of the island and location of the views. B: Pre-eruption IHM bathymetry. C: October 25, 2011. D: October 29, 2011. E: October 31, 2011. F: November 13, 2011. G: December 2, 2011. H: January 11, 2012. I: February 8, 2012. J: February 24, 2011. The eruptive center is indicated in C-J with a white arrow.

Figure S2. EK60 echograms recorded at frequencies of 38 kHz (left) and 120 kHz (right) during three stages of the eruption: October 29, 2011 (top), November 12, 2011 (middle) and February 23, 2012 (bottom). Vertical scales are in meters; color depicts volume backscattering coefficient (Sv) in decibels (dB) from red (max) to blue (min). Seabed displays the highest backscatter value and is marked also with a thin black line; below seafloor only artifacts (noise and multiples) are recorded. Within the water column, plumes of volcanic material are indicated. Intermediate backscatter below 300 m water depth in the high frequency record is static noise. Note the high backscatter layer around 400 m water depth in the low frequency records, which probably relates to a density boundary in the water column acting as a trap for light pyroclastic material.

Figure S3. General topo-bathymetric map of El Hierro Island, with the most recent bathymetric data in the eruption area. Locations of the new and older volcanic cones identified in El Hierro submarine and emerged edifice are shown. Histogram depicts the volumetric distribution of 221 submarine cones, with the 2011 eruption indicated as a reference. Number of submarine cones below $50 \cdot 10^6$ m^3 is probably underestimated, since they are barely

identifiable in the bathymetry. Debris avalanche scars and San Andrés fault system from Gee et al. (2001).

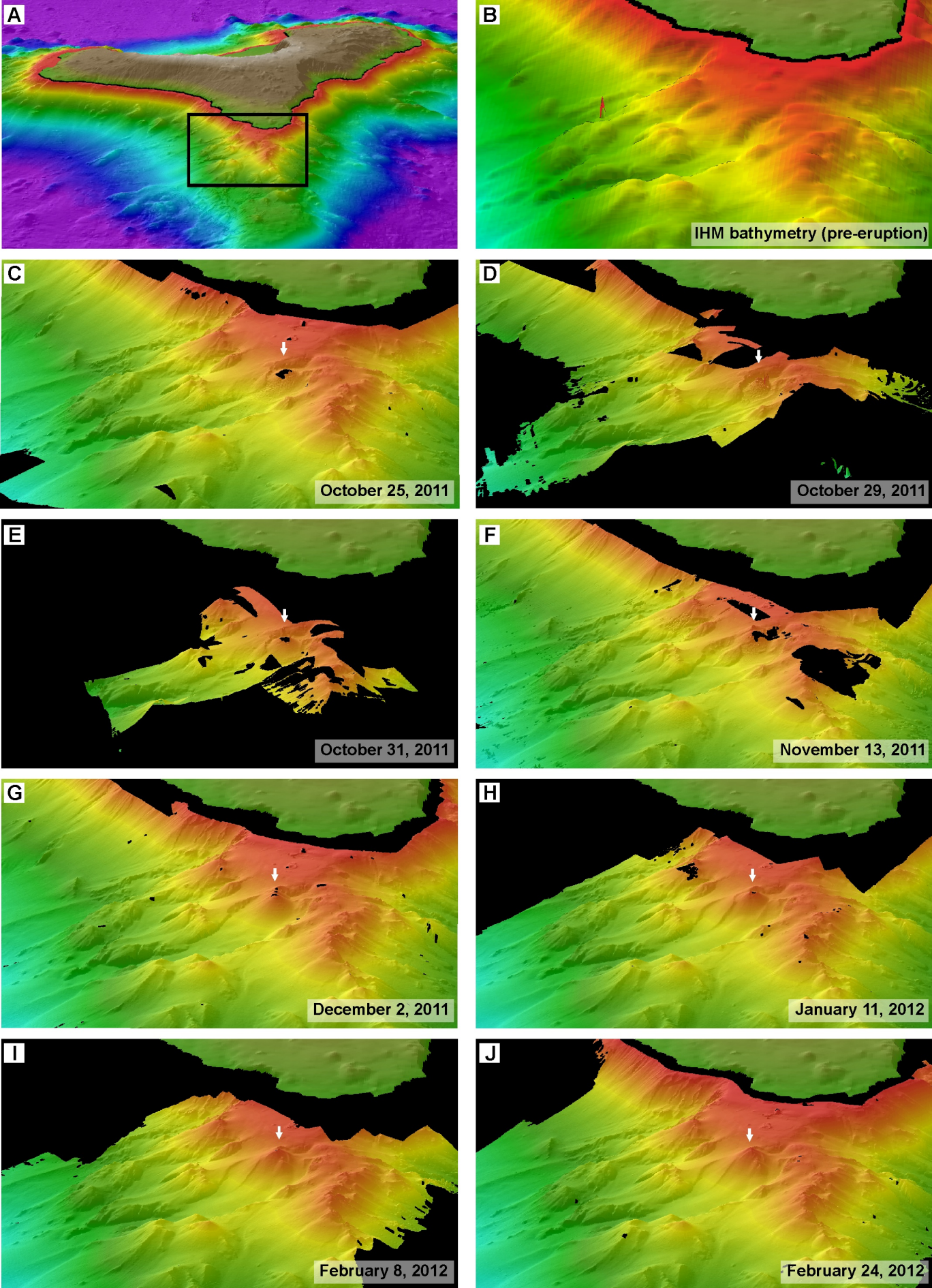
A
B
IHM bathymetry (pre-eruption)
C
October 25, 2011
D
October 29, 2011
E
October 31, 2011
F
November 13, 2011
G
December 2, 2011
H
January 11, 2012
I
February 8, 2012
J
February 24, 2012

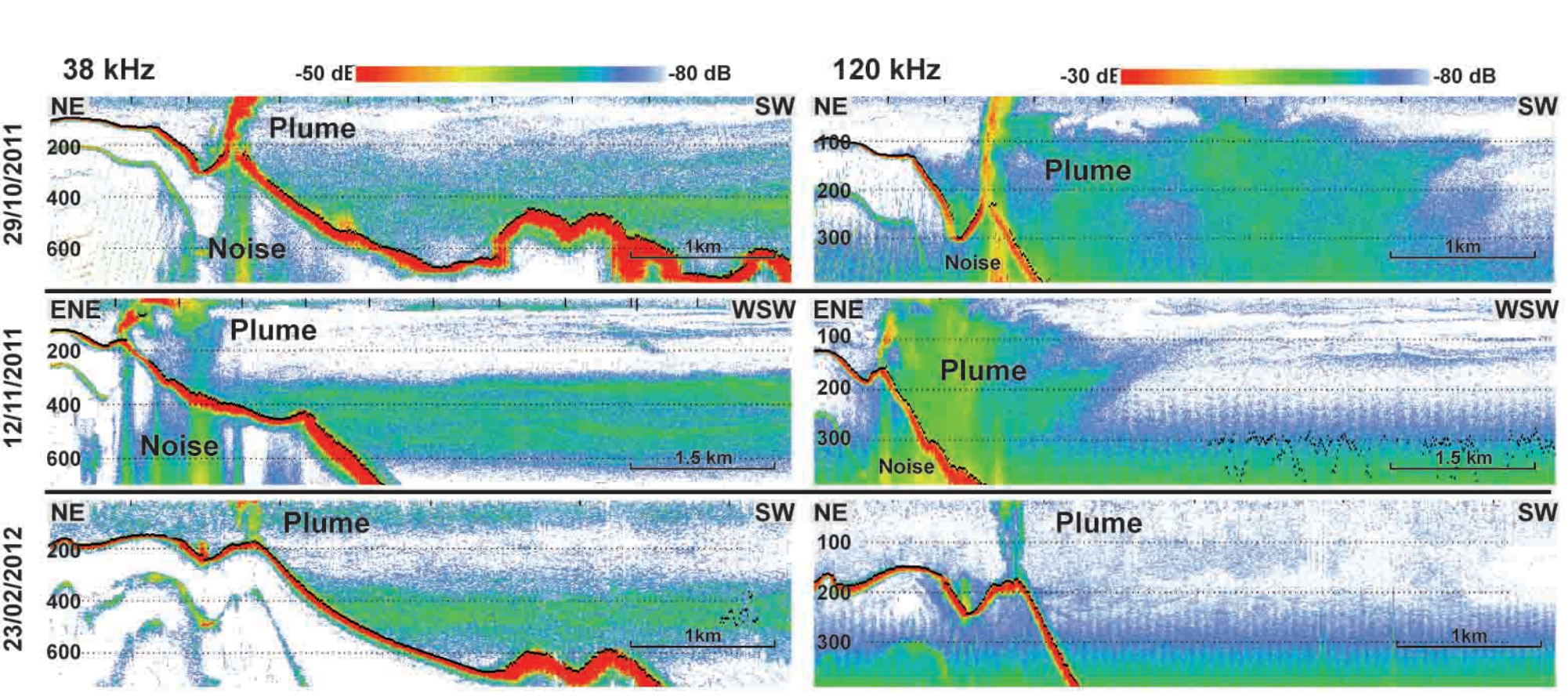
38 kHz
-50 dB
-80 dB
120 kHz
-30 dB
-80 dB
29/10/2011
12/11/2011
23/02/2012
NE
SW
ENE
WSW
Plume
Noise
200
400
600
100
300
1km
1.5 km

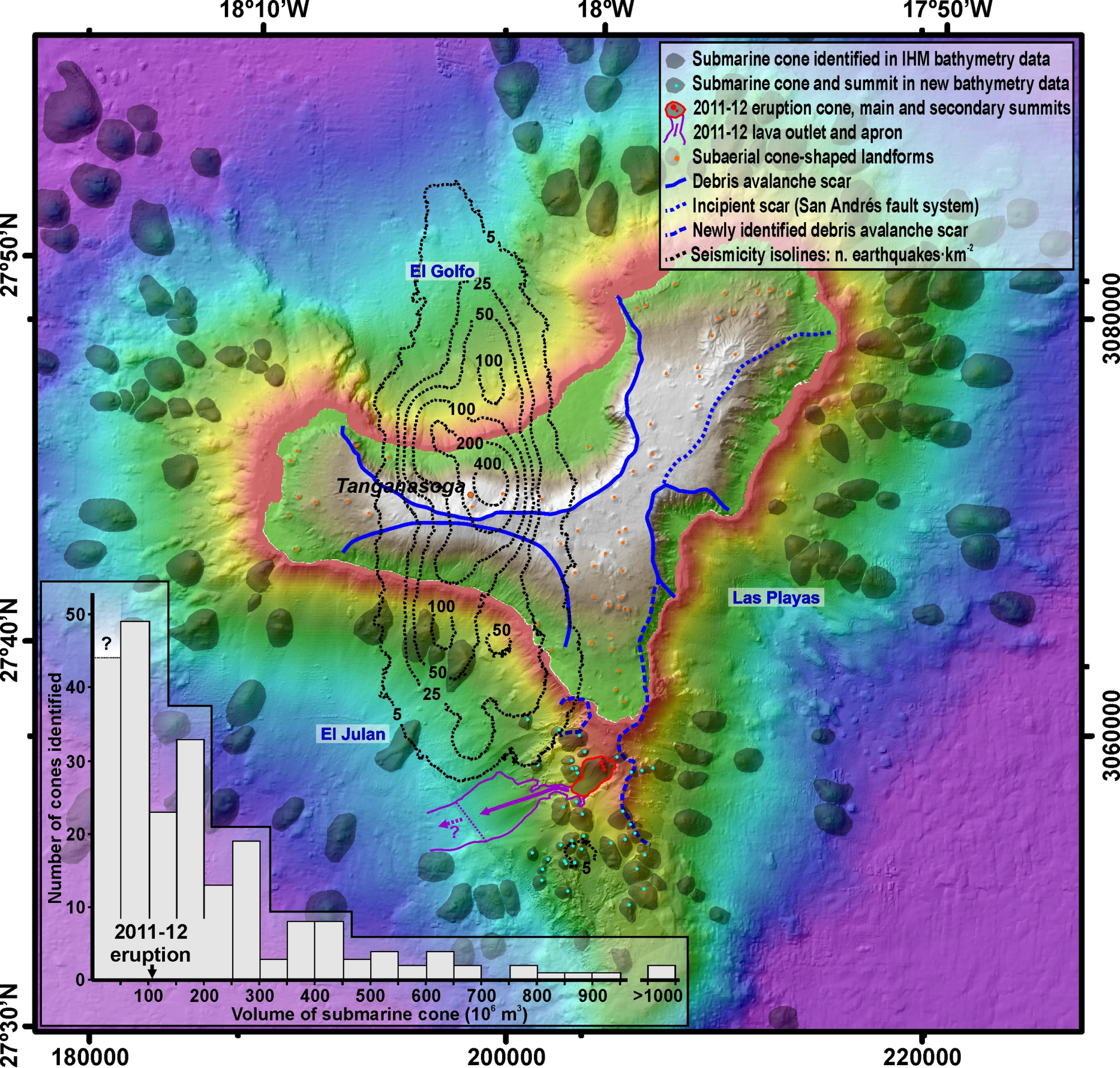
18°10'W
18°W
17°50'W
27°50'N
27°40'N
27°30'N
3080000
3060000
180000
200000
220000
Submarine cone identified in IHM bathymetry data
Submarine cone and summit in new bathymetry data
2011-12 eruption cone, main and secondary summits
2011-12 lava outlet and apron
Subaerial cone-shaped landforms
Debris avalanche scar
Incipient scar (San Andrés fault system)
Newly identified debris avalanche scar
Seismicity isolines: n. earthquakes·km-2
El Golfo
Tanganasoga
El Julan
Las Playas
5
25
50
100
200
400
Number of cones identified
Volume of submarine cone (10^6 m^3)
2011-12 eruption
?
>1000